



## Quantitative comparison between experimental and simulated gamma-ray spectra induced by 14 MeV tagged neutrons

B. Perot<sup>a,\*</sup>, W. El Kanawati<sup>a</sup>, C. Carasco<sup>a</sup>, C. Eleon<sup>a</sup>, V. Valkovic<sup>b</sup>, D. Sudac<sup>c</sup>, J. Obhodas<sup>c</sup>, G. Sannie<sup>d</sup>

<sup>a</sup> CEA, DEN, Cadarache, Nuclear Measurement Laboratory, F-13108 Saint-Paul-lez-Durance, France

<sup>b</sup> A.C.T.d.o.o., Prilesje 4, 10000 Zagreb, Croatia

<sup>c</sup> Ruder Boskovic Institute, Bijenicka c. 54, 10000 Zagreb, Croatia

<sup>d</sup> CEA, LIST, Saclay, F-91191 Gif-sur-Yvette, France

### ARTICLE INFO

Available online 18 July 2011

#### Keywords:

Fast neutron analysis

Associated particle technique

Explosive detection

Monte Carlo simulation

### ABSTRACT

Fast neutron interrogation with the associated particle technique can be used to identify explosives in cargo containers (EURITRACK FP6 project) and unexploded ordnance on the seabed (UNCOSS FP7 project), by detecting gamma radiations induced by 14 MeV neutrons produced in the  $^2\text{H}(^3\text{H},\alpha)\text{n}$  reaction. The origin of the gamma rays can be determined in 3D by the detection of the alpha particle, which provides the direction of the opposite neutron and its time-of-flight. Gamma spectroscopy provides the relative counts of carbon, nitrogen, and oxygen, which are converted to chemical fractions to differentiate explosives from other organic substances. To this aim, Monte Carlo calculations are used to take into account neutron moderation and gamma attenuation in cargo materials or seawater. This paper presents an experimental verification that C, N, and O counts are correctly reproduced by numerical simulation. A quantitative comparison is also reported for silicon, iron, lead, and aluminium.

© 2011 Elsevier Ltd. All rights reserved.

### 1. Introduction

Fast neutron interrogation can be used in a variety of areas (Buffler and Tickner, 2010) to identify materials, especially for explosive detection. The associated particle technique (Valkovic et al., 1969) has been applied in EU projects like EURITRACK, Eritr@C, and UNCOSS, in which extensive databases of gamma-ray signatures induced by 14 MeV neutrons on individual elements (C, N, O, Na, Al, Si, Cl, K, Ca, Cr, Fe, Ni, Cu, Zn, Pb, etc.) have been produced and compared to MCNP simulations (Perot et al., 2008; El Kanawati et al., 2011a,b). Attention has been focused on main peaks and neutron scattering continuum, showing a satisfactory qualitative agreement for C, N, and O spectra used for explosive identification. The gamma-ray spectrum of an unknown interrogated material is fitted with a linear combination of these elemental signatures to determine their relative count fractions, which are then converted to chemical proportions taking into account gamma-ray production cross sections for the neutron energy spectrum reaching the target materials, and photon attenuation between the target and gamma-ray detectors (Carasco et al., 2007). This reference reports an approach mixing Monte Carlo simulation of neutron transport and gamma energy deposition in the detector with analytical calculation of photon attenuation. A new approach

entirely based on Monte Carlo simulation is now possible, thanks to recent developments in MCNP output file processing (Carasco, 2010), allowing realistic time–energy resolution and counting statistics descriptions. New sets of correction factors are being produced within Eritr@C (because EURITRACK's low-energy threshold was reduced from 1.35 to 0.6 MeV to improve the detection of some elements; El Kanawati et al., 2010) and UNCOSS projects. MCNPX RSICC has been used, instead of MCNP 4C in (Carasco et al., 2007), and the ENDF/B-VII.0 data library instead of ENDF/B-VI.0. Results will be reported soon, the aim of this paper being to verify that numerical simulation quantitatively reproduces the counts in gamma-ray spectra of well-known samples of graphite (for carbon), water (for oxygen), and melamine ( $\text{C}_3\text{H}_6\text{N}_6$  for nitrogen and carbon). Comparisons for other materials frequently found in cargo containers (Obhodas et al., 2010) or part of the EURITRACK portal are also presented: wood ( $\text{C}_{22}\text{H}_{31}\text{O}_{12}$ ), silicon dioxide sand, aluminium, iron, and lead blocks.

The gamma-ray production cross sections reported in Simakov et al. (1998) indeed show large discrepancies between experimental data, and inconsistencies in the evaluated data libraries like ENDF/B-V and ENDF/B-VI have also been observed (Bendahan et al., 1995), even for well-known elements like C, N, and O. The ENDF/B-VI.0 database used in Carasco et al. (2007) also did not reproduce the anisotropic gamma-ray production, contrary to ENDF/B-VII.0, which is of importance when inspecting different areas inside a cargo container with a large variety of beam-to-detector angles.

\* Corresponding author. Tel.: +33 442254048; fax: +33 442252367.  
E-mail address: [bertrand.perot@cea.fr](mailto:bertrand.perot@cea.fr) (B. Perot).

## 2. Experiment vs. MCNP simulation

The samples described in Table 1 have been measured with the geometry shown in Fig. 1.

The pyramidal tagged neutron beam has been modelled with the conical source of MCNP, which has been shaped to the square experimental beam with a frame selecting only the neutrons in the appropriate solid angle. The neutron-induced photon flux is estimated using “point detectors” (MCNP type 5 tally) located above the target, between the two parallel rows of EURITRACK top detectors. The photon flux is then used as a source in a second calculation of their energy deposition in the NaI(Tl)  $5'' \times 5'' \times 10''$  detectors, using the MCNP “pulse height tally” (F8). In this second calculation, the photons are injected under a normal incidence in the small face ( $5'' \times 5''$ ) of the detectors. MODAR software is used to fasten this two-step calculation by implementing pre-calculated response functions of the detector based on F8 calculations taking into account the energy resolution observed experimentally (Carasco, 2010). To limit the bias due to incidence angle, only the three pairs of top detectors located above the target have been used.

The neutron time-of-flight (TOF) spectrum of the graphite sample acquisition is shown in Fig. 2 (top panels). The random background observed in the negative times has been subtracted from the other areas of interest. The first peak near 10 ns is due to tagged neutron interactions in the walls of the generator and

surrounding materials. The main peak due to graphite centred at about 31 ns overlaps with a smaller signal due to tagged neutrons scattered by the sample towards the NaI(Tl) detectors, surrounding iron structures and lead collimators. Selecting the graphite TOF window provides the expected gamma spectrum of carbon (middle, left panel), with its full-energy and escape peaks, whereas the scattered neutron spectrum (middle, right panel) does not reveal noticeable gamma signature. The fraction of scattered neutron signal overlapping in the graphite TOF window has been estimated to be 16% using Gaussian functions (top, right panel), and it has been subtracted to obtain the net carbon spectrum (bottom panel).

The agreement between experiment and MCNP is satisfactory, taking into account the following sources of uncertainty, which will also apply for all further samples.

1. Fig. 2 shows significant statistical fluctuations due to limited acquisition time in Rijeka seaport, where the EURITRACK system is under operation (Carasco et al., 2008), and to the use of only six detectors above the target to limit the gamma angle of incidence.
2. Systematic uncertainties must also be taken into account, of which the most important is certainly the precision of the nuclear data used in MCNP. Relative standard deviations of the experimental data reported in Simakov et al. (1998) are generally 10–20%, but they are much larger for a number of gamma rays. As already mentioned the construction of evaluated nuclear data files also suffers from proper uncertainties (Carasco et al., 2008).
3. Modelling and calculation methods introduce uncertainties in the geometry and material descriptions. The injection of the photon flux perpendicular to the detector entrance surface to calculate energy deposition is an example of modelling approximation.
4. Count losses in the data acquisition system can be a source of uncertainty but the alpha–gamma coincidence rate was only about  $3000 \text{ s}^{-1}$ . The EURITRACK front-end electronics dead-time being close to  $5 \mu\text{s}$ , essentially due to the QDC conversion time (Lunardon et al., 2007), count losses are lower than 1.5%.
5. A filtering algorithm is used to suppress multiple alpha or gamma hits, and other unwanted events. The filtering ratio of good to total events is significant, typically 50%, and only good events have been used to scale calculation for a quantitative comparison with experiment. However a fraction of the rejected

**Table 1**  
Characteristics of the modelled experiments.

Target	Source to target distance (cm)	Target to detector distance (cm)	Density	Dimensions		
				X (cm)	Y (cm)	Z (cm)
Graphite	104	89	1.75	20	30.1	20
Water	103	96	1	25	14	14
Lead	95	100	11.2	5	20	40
Iron	96	97	7.4	1	41	44.5
Melamine	95	89	0.95	15	20	10
Wood	101	91	0.6	46	40	17
Silicon dioxide	85	93	1.75	15	20	6
Aluminium	94.5	100	2.66	Diameter=20 cm		22.5

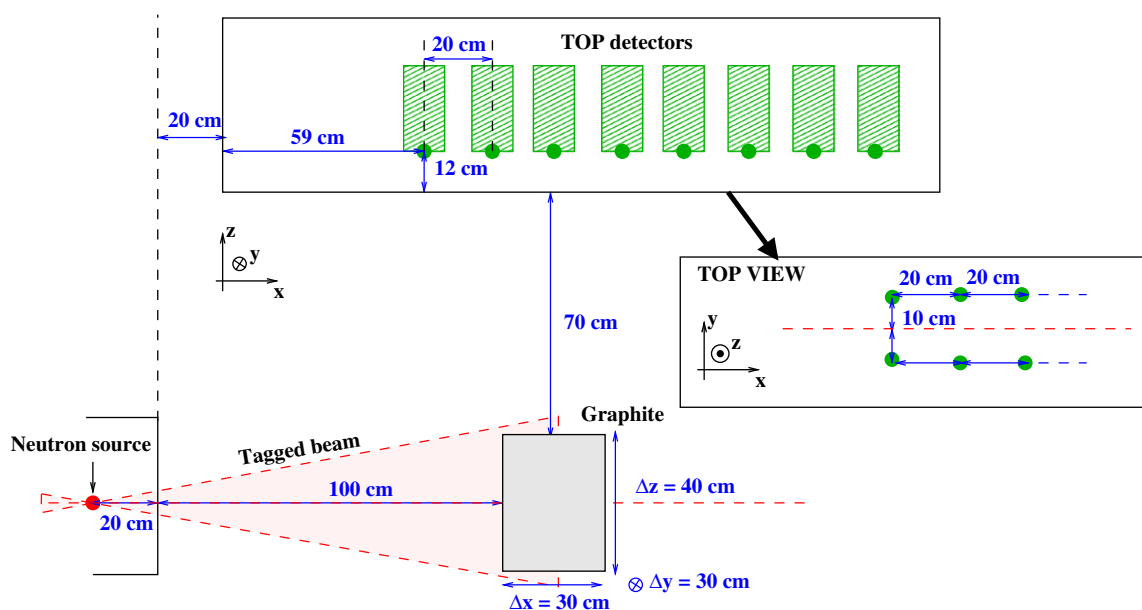


**Fig. 1.** Setup of the graphite target acquisition. The points below the  $5'' \times 5'' \times 10''$  NaI(Tl) top detectors represent the location of the MCNP point detectors.

Download English Version:

<https://daneshyari.com/en/article/1876132>

Download Persian Version:

<https://daneshyari.com/article/1876132>

[Daneshyari.com](https://daneshyari.com)